

# Inspection of $^{56}\text{Fe}$ $\gamma$ -Ray angular distributions as a function of incident neutron energy using optical model approaches

J.R. Vanhoy<sup>1,3,a</sup>, A.P. Ramirez<sup>2,b</sup>, D.K. Alcorn-Dominguez<sup>1</sup>, S.F. Hicks<sup>3,c</sup>, E.E. Peters<sup>2</sup>, M.T. McEllistrem<sup>2</sup>, S. Mukhopadhyay<sup>2</sup>, and S.W. Yates<sup>2,4</sup>

<sup>1</sup> Department of Physics, U.S. Naval Academy, 21666 Annapolis, Maryland, USA

<sup>2</sup> Department of Chemistry, University of Kentucky, 40506 Lexington, Kentucky, USA

<sup>3</sup> Department of Physics, University of Dallas, 75062 Irving, Texas, USA

<sup>4</sup> Department of Physics & Astronomy, University of Kentucky, 40506 Lexington, Kentucky, USA

**Abstract.** Neutron inelastic scattering cross sections measured directly through (n,n) or deduced from  $\gamma$ -ray production cross sections following inelastic neutron scattering (n,n' $\gamma$ ) are a focus of basic and applied research at the University of Kentucky Accelerator Laboratory ([www.pa.uky.edu/accelerator](http://www.pa.uky.edu/accelerator)). For nuclear data applications, angle-integrated cross sections are desired over a wide range of fast neutron energies. Several days of experimental beam time are required for a data set at each incident neutron energy, which limits the number of angular distributions that can be measured in a reasonable amount of time. Approximations can be employed to generate cross sections with a higher energy resolution, since at 125°, the  $a_2P_2$  term of the Legendre expansion is identically zero and the  $a_4P_4$  is assumed to be very small. Provided this assumption is true, a single measurement at 125° would produce the  $\gamma$ -ray production cross section. This project tests these assumptions and energy dependences using the codes CINDY/SCAT and TALYS/ECIS06/SCAT. It is found that care must be taken when interpreting  $\gamma$ -ray excitation functions as cross sections when the incident neutron energy is < 1000 keV above threshold or before the onset of feeding.

## 1. Introduction

Neutron-induced reactions are the main research activity at the University of Kentucky Accelerator Laboratory (UKAL). Neutrons are produced by impinging a pulsed beam of protons or deuterons into a gas cell containing either tritium or deuterium. Samples are hung  $\sim 7$  cm from the gas cell. Scattered neutrons or  $\gamma$  rays are registered in appropriate detectors mounted inside collimated shielding on a moveable carriage. The time-of-flight (TOF) technique allows for measurement of the scattered neutron energies and for background suppression. Three types of measurements are typically performed and are illustrated in Fig. 1.

Inelastic neutron (n,n') scattering angular distributions are measured for scattered angles of 30° to 155° at fixed incident neutron energies ( $E_n$ ). There are numerous advantages for using this technique to obtain inelastic cross sections. The incident beam contains only a single neutron energy and therefore the inelastic cross section to a given final state is measured directly without feeding complications. The neutron angular distribution contains details about the reaction mechanism not discoverable with angle-integrated techniques. There are several disadvantages to the (n,n') technique. Usually only the first few excited states occur as isolated peaks in the spectrum with the higher-lying final levels unresolved.

The count rate is low for neutron detection with TOF, so individual spectra take 4–8 hours each. Three to four days are required to measure each angular distribution, and this limits the number that can be completed in the allotted beam time.

Gamma-ray (n,n' $\gamma$ ) angular distributions are measured for scattered angles of 30° to 155° at fixed incident neutron energies ( $E_n$ ). There are also numerous advantages for using this technique to discover inelastic cross sections. The incident beam contains only a single neutron energy and while the raw yield of a particular  $\gamma$  ray may be impacted by feeding from higher-lying states, the feeding contribution can be subtracted since it is directly measured. The energy resolution of HPGe detectors is excellent, so that cross sections can be determined to all excited final states. In addition, the  $\gamma$ -ray data contain nuclear structure information such as spins and parities, branching ratios, mixing ratios, lifetimes, and electromagnetic transition rates. Two to three days are required to measure a high-quality angular distribution, limiting the number that can be completed in the allotted beam time.

The third technique to determine inelastic cross sections is to measure the  $\gamma$ -ray excitation function. The detector is placed at 125° and spectra are taken as the incident neutron energy is stepped upward. Again, only one incident neutron energy is present and any feeding is observed and easy to subtract. The HPGe has excellent energy resolution and spectra are reasonably quick to obtain. Angle-integrated cross sections for the complete region of interest can be obtained with a week of beam

<sup>a</sup> e-mail: [vanhoy@usna.edu](mailto:vanhoy@usna.edu)

<sup>b</sup> e-mail: [ap.ramirez@uky.edu](mailto:ap.ramirez@uky.edu)

<sup>c</sup> e-mail: [hicks@udallas.edu](mailto:hicks@udallas.edu)

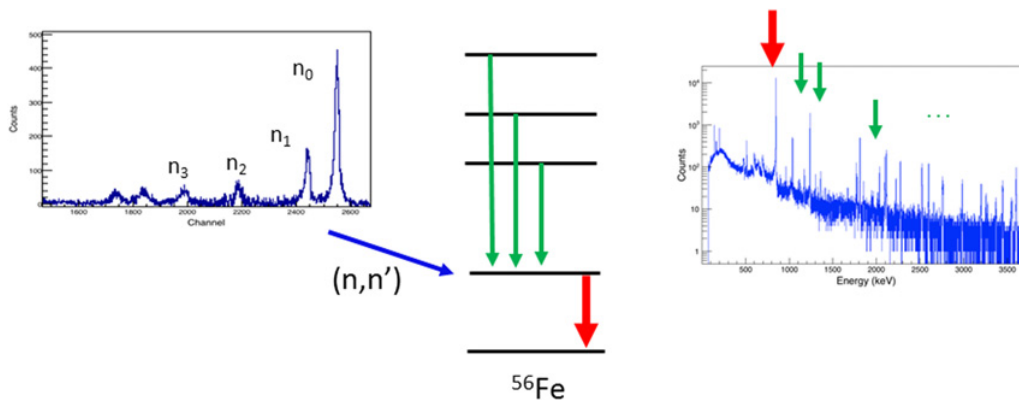


**Figure 1.** Inelastic scattering cross sections to individual final states may be determined by measuring the scattered neutrons or by observing  $\gamma$ -ray emission from the final state and subtracting the cross sections of feeding transitions.

**Table 1.** Constraints on the  $a_4$  Legendre coefficient in determining acceptable values of the inelastic cross section from a  $125^\circ$  measurement.

Desired Error	Allowable $ a_4 $
< 1%	< 0.0260
< 2%	< 0.0519
< 3%	< 0.0779
< 5%	< 0.1298

time. This technique requires that the  $a_4 P_4$  term in each  $\gamma$ -ray's angular distribution at  $125^\circ$  be negligible. This paper examines this assumption.

## 2. Calculations

Gamma-ray angular distributions involving multipolarities  $L = 1$  and  $2$  are written as a Legendre polynomial expansion:  $W(\theta_\gamma) = A_0 [1 + a_2 P_2(\theta_\gamma) + a_4 P_4(\theta_\gamma)]$ , where  $P_L$  are the Legendre polynomials. Higher-order terms do not occur for dipole and quadrupole transitions. The quantity  $4\pi A_0$  is the angle-integrated  $\gamma$ -ray production cross section when properly normalized.

Table 1 presents maximum allowable  $a_4$  coefficients for various limits of error. In a situation where the discrepancy is  $\sim 5\%$ , the error is comparable to the uncertainties arising from multiple scattering corrections or the cross section normalization and will have an impact upon the accuracy of the cross section reported. If the discrepancy is  $\leq 2\%$ , the error is minor and does not significantly impact reported cross section values.

The Legendre coefficients are derived with angular momentum algebra treatments such as that presented in Ferguson [1]. The  $a_2$  and  $a_4$  coefficients are controlled by the upper and lower state spins and the substate population distribution of the upper state. The substate population distribution is referred to as the alignment and often considered to be a Gaussian distribution about  $m_J = 0$ , with spreading width  $\sigma$ . The upper level's alignment is determined by entrance and exit channel transmission coefficients (and angular momentum coupling).

In this investigation, we explore the  $\sigma$  spreading width and  $a_4$  values using: 1) the der Mateosian, Sunyar [2], and Yamazaki [3] (MSY) Atomic Data and Nuclear Data Tables tables, 2) the Hauser-Feshbach code CINDY [4,5] with either an optical model parameter set or  $T_{ij}$  transmission coefficients from TALYS [6], and 3) experimental measurements of  $\gamma$ -ray angular distributions.

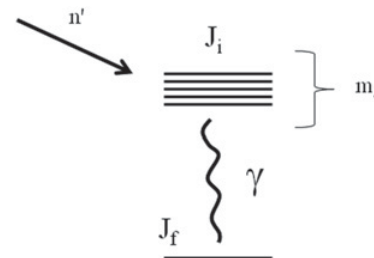


**Figure 2.** Formation and de-excitation of a level in the residual nucleus. The transmission coefficients  $T_{ij}$  of the exit channel neutrons from the final level and determine the probability distribution of the  $m_J$  substates. In turn, the  $m_J$  populations strongly influence the  $\gamma$ -ray angular distribution.

**Table 2.** Substate spreading, alignment  $\sigma$ , attenuation factors  $\alpha$ , and Legendre coefficients using the MSY tables.

$\sigma/J$	$\sigma$	Attenuation factors			
		$\alpha_2$	$\alpha_4$	$a_2$ ( $\times 10^3$ )	$a_4$ ( $\times 10^3$ )
0	0	1	1	714	-1714
0.2	0.4	0.959	0.865	685	-1484
0.4	0.8	0.683	0.202	488	-346
0.5	1.0	0.538	0.0952	384	-163
0.6	1.2	0.415	0.0484	296	-083
0.7	1.4	0.322	0.0266	230	-046
0.8	1.6	0.255	0.0157	181	-027
1.0	2.0	0.168	0.00641	120	-011

### 2.1. MSY tables

The tables of der Mateosian, and Sunyar [2], and Yamazaki [3] (MSY) may be used to 'fit'  $\gamma$ -ray angular distributions if computer codes are not available to perform the angular momentum algebra. This approach is an empirical technique, where decays from known levels are used to judge the appropriate value of  $\sigma$ . This  $\sigma$  is assumed valid for the alignment of near-by states. Table 2 provides an example for  $2^+ \rightarrow 0^+$  decays.

We see from Table 2 that the 5% discrepancy limit is reached when  $\sigma \sim 1.1$  and the 2% discrepancy limit is reached when  $\sigma \sim 1.4$ .

### 2.2. CINDY

To understand when certain values of  $\sigma$  are expected in actual excitation function measurements, we utilize

**Table 3.** Substate populations, Legendre Coefficients for the decay of the 847-keV  $2^+$  state in  $^{56}\text{Fe}$  using optical model parameters as discussed in the text.

$E_n$ (MeV)	$\sigma$	$a_2$ ( $\times 10^3$ )	$a_4$ ( $\times 10^3$ )
0.9	0.83	511	-310
1.0	0.88	452	-256
1.5	1.04	306	-149
2.0	1.17	244	-103
2.5	1.28	205	-078
3.0	1.36	187	-065
3.5	1.38	179	-063
4.0	1.40	170	-061
4.5	1.43	158	-059
5.0	1.48	144	-054

**Table 4.** Substate populations, Legendre Coefficients for the decay of the 847-keV  $2^+$  state in  $^{56}\text{Fe}$  using transmission coefficients  $T_{ij}^{\pm}$  generated by TALYS.

$E_n$ (MeV)	$\sigma$	$a_2$ ( $\times 10^3$ )	$a_4$ ( $\times 10^3$ )
1.5	1.01	306	-167
2.0	1.20	221	-101
2.5	1.35	185	-068
3.0	1.43	171	-054
3.5	1.46	170	-051
4.0	1.46	166	-052
4.5	1.47	157	-052
5.0	1.51	145	-049

the code CINDY [4,5] to predict alignments and  $a_2$  and  $a_4$  coefficients for the first excited state of  $^{56}\text{Fe}$  as a function of incident neutron energy. CINDY performs a Hauser-Feshbach reaction model calculation and handles the angular momentum algebra. One must provide either optical model potential parameters or transmission coefficients as a function of neutron energy. We have examined both approaches.

Table 3 provides the alignment and Legendre coefficients obtained when a simplified version of the Koning & Delaroche [7] neutron optical model parameters are used. At a fundamental level, CINDY calculates transmission coefficients using the subroutine SCAT [8], the same base routine employed in TALYS/ECIS and performs Moldauer fluctuation corrections. The optical model treatment in CINDY is not sophisticated by today's standards and values for the cross sections are not the best, but the code does handle the angular momentum calculations rather well. The  $\sigma$  was estimated by comparing the  $m_j = 0$  and  $m_j = 1$  substate population probabilities using  $P(m_j) \sim \exp(-m_j^2/2\sigma^2)$ . The substate population distributions are not perfectly Gaussian at  $> 2$  MeV above threshold.

In Table 3, we observe that even at threshold for exciting the  $2_1^+$  level, the substates are not fully aligned. The 5% discrepancy limit is reached at  $E_n \sim 1.8$  MeV – or  $\sim 900$  keV above the threshold for exciting the  $2_1^+$ . The 2% discrepancy limit is reached at  $E_n \sim 5.0$  MeV – or  $\sim 4.0$  MeV above the threshold.

Table 4 provides the alignment and Legendre coefficients obtained from TALYS. TALYS is a full-featured code which uses a sophisticated optical model

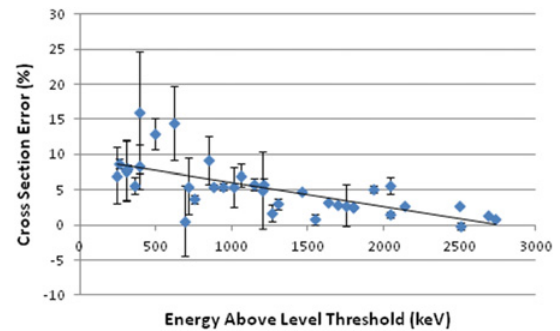


**Figure 3.** Collected  $a_4$  coefficients from angular distribution measurements on numerous Ce, Nd, Te, Fe isotopes.

treatment, incorporates all open channels, and can apply numerous refinements to obtain higher-quality transmission coefficients. TALYS produces quality values for cross sections but does not calculate  $\gamma$ -ray angular distributions. Hence the  $T_{ij}^{\pm}$  transmission coefficients generated by TALYS were inserted into CINDY to manage the angular momentum algebra.

From Table 4 we observe that the 5% discrepancy limit is reached at  $E_n \sim 1.8$  MeV – or  $\sim 900$  keV above the threshold for exciting the  $2_1^+$ . The 2% discrepancy limit is reached at  $E_n \sim 2.8$  MeV – or  $\sim 2000$  keV above the threshold.

### 2.3. Experimental measurements

Values in Tables 3 and 4 do not include the additional spreading of  $\sigma$  that would result from  $\gamma$ -ray feeding from higher-lying states. This additional effect becomes significant a couple of MeV above the  $2_1^+$  level. Attempts to take this into account with calculations are too labor-intensive and would be too ambiguous because of uncertainties in the higher state alignments and multipole mixing ratios for their decays. To gauge the experimental reality, we compile information from numerous  $2_i^+ \rightarrow 0^+$  angular distribution measurements at the UKAL on many nuclei over the last 30 years. Figure 3 displays the measured  $a_4$  coefficients as a function of energy above the threshold for the level. The trendline indicates the  $< 5\%$  limit is reached about 1000 keV above threshold and the  $< 2\%$  limit  $\sim 2000$  keV above threshold. This observation is consistent with our CINDY predictions for the  $^{56}\text{Fe}$   $2_1^+$ , and suggests the same will be true for all  $2^+ \rightarrow 0^+$  transitions.

## 3. Summary

Transmission coefficients for  $l = 0, 1, 2$  channels have significant differences depending on the reaction model treatment used. This variation impacts the overall scale of the cross sections but not so much the  $\gamma$ -ray angular distributions.

Ignoring the  $a_4P_4$  term in the angular distribution creates serious discrepancies for  $2_i^+ \rightarrow 0^+$  transitions before the onset of feeding. The  $a_4P_4$  discrepancy is not as important for other spin states,  $J = 3, 4, \dots$  because substate spreadings  $\sigma$  are wider and therefore large  $a_4$  values tend not to occur.

Substate spreading differs slightly according to the choice of optical model treatment, but the impact upon the  $\gamma$ -ray angular distribution is not large.

Care must be taken when interpreting  $\gamma$ -ray excitation functions as cross sections when 1) the incident neutron energy is  $< 1000$  keV above threshold or 2) before the onset of feeding.

This work is supported by the Department of Energy National Nuclear Security Administration under Award Number DE-NA0002931.

## References

- [1] A.J. Ferguson, *Angular Correlation Methods in Gamma-Ray Spectroscopy* (North-Holland, Amsterdam, 1965)
- [2] E. der Mateosian and A.W. Sunyar, *At. Data and Nucl. Data Tables* **13**, 391 (1974)
- [3] T. Yamazaki, *Nucl. Data* **A3**, 1 (1967)
- [4] E. Sheldon and D.M. van Patter, *Rev. Mod. Phys.* **38**, 143 (1966)
- [5] E. Sheldon and V.C. Rogers, *Comp. Phys. Comm.* **6**, 99 (1971)
- [6] A.J. Koning, S. Hilaire, and M.C. Duijvestijn, TALYS1.0, *Proceedings of the International Conference on Nuclear Data for Science and Technology - ND2007* (EDP Sciences, 2008) 211–214
- [7] A.J. Koning and J.P. Delaroche, *Nucl. Phys. A* **713**, 231 (2003)
- [8] W.R. Smith, *Comp. Phys. Comm.* **1**, 106 (1969)